UC San Diego
UC San Diego Previously Published Works

Title
Localizing Age-Related Changes in Brain Structure between Childhood and Adolescence Using Statistical Parametric Mapping

Permalink
https://escholarship.org/uc/item/6ww6h4zd

Journal
NeuroImage, 9(6)

ISSN
1053-8119

Authors
Sowell, Elizabeth R
Thompson, Paul M
Holmes, Colin J
et al.

Publication Date
1999-06-01

DOI
10.1006/nimg.1999.0436

Peer reviewed

Localizing Age-Related Changes in Brain Structure between Childhood and Adolescence Using Statistical Parametric Mapping

Elizabeth R. Sowell,*,† Paul M. Thompson,* Colin J. Holmes,* Rajneesh Batth,*
Terry L. Jernigan,‡ and Arthur W. Toga*

*Department of Neurology, Laboratory of Neuroimaging, and †Division of Child and Adolescent Psychiatry, University of California at Los Angeles, Los Angeles, California 90095; and ‡Department of Veterans Affairs Medical Center and Departments of Psychiatry and Radiology, University of California, San Diego, School of Medicine, San Diego, California

Volumetric studies have consistently shown reductions in cerebral gray matter volume between childhood and adolescence, with the most dramatic changes occurring in the more dorsal cortices of the frontal and parietal lobes. The purpose of this study was to examine the spatial location of these changes employing methods typical of functional imaging studies. T_1-weighted structural MRI data (1.2 mm) were analyzed for nine normally developing children and nine normal adolescents. Validity and reliability of the tissue segmentation protocol were assessed as part of several preprocessing analyses prior to statistical parametric mapping (SPM). Using SPM96, a simple contrast of average gray matter differences between the two age groups revealed 57 significant clusters (SPM{Z} height threshold, $P < 0.001$, extent threshold 50, uncorrected). The pattern and distribution of differences were consistent with earlier findings from the volumetric assessment of the same subjects. Specifically, more differences were observed in dorsal frontal and parietal regions with relatively few differences observed in cortices of the temporal and occipital lobes. Permutation tests were conducted to assess the overall significance of the gray matter differences and validity of the parametric maps. Twenty SPMs were created with subjects randomly assigned to groups. None of the random SPMs approached the number of significant clusters observed in the age difference SPM (mean number of significant clusters = 5.8). The age effects observed appear to result from regions that consistently segment as gray matter in the younger group and consistently segment as white matter in the older group. The utility of these methods for localizing relatively subtle structural changes that occur between childhood and adolescence has not previously been examined. © 1999 Academic Press

Key Words: myelination; normal development; MRI.

INTRODUCTION

Studies of normal brain maturation (Jernigan *et al.,* 1991; Pfefferbaum *et al.,* 1994; Caviness *et al.,* 1996; Giedd *et al.,* 1996a,b; Reiss *et al.,* 1996; Sowell and Jernigan, 1999; Sowell *et al.,* submitted for publication) have consistently shown that brain morphology changes dynamically into adulthood. Gray matter volume reductions between childhood and adolescence with relatively stable total brain volume in this age range have been consistent findings in the literature. This would be expected given postmortem studies that have revealed a protracted progression of myelination, particularly into frontal and parietal regions (Yakovlev and Lecours, 1967) continuing well into the third decade of life. Additionally, regressive events, such as reductions in synaptic density, have been reported to occur throughout adolescence in humans (Huttenlocher, 1979; Huttenlocher and de Courten, 1987) and in monkeys (Zecevic and Rakic, 1991). These studies show that maturational factors occur in a programmed way such that more primitive regions of the brain (e.g., brain stem, cerebellum) mature earlier, and phylogenetically more advanced regions of the brain (e.g., association cortices of the frontal lobes) develop later.

In a detailed *in vivo* study of human brain maturation, Sowell *et al.* (submitted for publication) reported evidence for a subtle increase in total cerebral volume between the ages of 7 and 16 years. Brain size-corrected measures of overall white matter also showed evidence for an increase with age, while measures of total cortical gray matter (corrected for total brain volume) significantly decreased with age. More dramatic cortical change appeared to be occurring in frontal and parietal regions during this age range with highly significant reductions in gray matter and concomitant increases in white matter. Subcortical structures did not appear to be changing as much with significant volume reductions observed only in the thalamus and

trend level reductions in the caudate nuclei. Cerebrospinal fluid (CSF) volume increases were observed adjacent to the frontal and lateral temporal cortices, but these changes were quite subtle relative to the cortical gray and white matter age effects. Generally, the *in vivo* findings reflect the pattern of change observed in postmortem studies (e.g., Yakovlev and Lecours, 1967) where maturational phenomena progress from inferior to superior regions and posterior to anterior regions.

While volumetric studies have provided some evidence for regional specificity of maturational changes, the question of spatial localization of brain development between childhood and adolescence has not been addressed in the literature. Such information could provide further insight into the functional significance of regionally specific maturation in healthy children. For example, volumetric studies show reductions in gray matter with concomitant increases in white matter and CSF within the frontal lobes, but the exact histological underpinnings of these changes are not known. Clearly we can infer from our knowledge of postmortem studies that myelin deposition is continuing and regressive events are occurring, but which is most responsible for the volumetric changes we observe? With *in vivo* volumetric studies, scientists are somewhat limited in their localization abilities because the boundaries of gross anatomical structures can be ambiguous and time consuming to define in great detail. Methods that are traditionally used to assess functional imaging data may be useful, and perhaps more efficient, in localizing the age effects observed in the volumetric studies. With statistical parametric mapping (SPM) techniques, the whole brain can be analyzed at once without tedious slice by slice region definition. A similar approach was first reported by Andraesen *et al.* (1994) where structural differences in schizophrenia were examined on a voxel by voxel basis.

The goal of this study was to further explore maturational changes in the developing human brain using statistical parametric mapping techniques (SPM96; Friston *et al.,* 1995). A subset of the children and adolescents studied earlier by Sowell *et al.* (submitted for publication) was also studied here, and predictions were made that age-related changes observed in this study would parallel the pattern observed in the volumetric assessment of these children. Specifically, it was predicted that more age effects would be localized in the dorsal cortices of frontal and parietal lobes, while relatively few age effects would be observed in the ventral cortices of the temporal lobes and in the subcortical space.

METHODS

Subjects. Nine children (7 to 10 years; mean age 8.6 years; 5 boys, 4 girls) and 9 adolescents (12 to 16 years; mean age 14 years; 5 boys, 4 girls) were examined with SPM. Another group including 19 subjects (15 of whom were also assessed in the SPM analyses) were assessed for validation of the tissue segmentation methods. All subjects were recruited as normal controls for a large, multidisciplinary neurodevelopmental research center. All of the children were right handed and each was screened for neurological impairments and for any history of learning disability or developmental delay. Informed consent was obtained from all children and their parents.

Imaging protocol. Three whole-brain image series were collected for each subject. The first was a gradient-echo (SPGR) T_1-weighted series with TR = 24 ms, TE = 5 ms, NEX = 2, flip angle = 45°, field of view of 24 cm, section thickness of 1.2 mm, no gaps (shown in Fig. 1). The second and third series were a fast spin-echo acquisition yielding two separate image sets: TR = 3000 ms, TE = 17 ms, ET = 4 and TR = 3800 ms, TE = 102 ms, ET = 8; for both sets the field of view was 24 cm, section thickness 4 mm, no gaps (interleaved). Imaging time for both series totaled approximately 30 min.

Image processing. Image data sets were subjected to the following preprocessing analyses: reslicing of the volume into a standard orientation, interactive isolation of supratentorial cranial regions from surrounding extracranial and infratentorial tissue, three-dimensional digital filtering to reduce inhomogeneity artifact (Sled *et al.,* 1998), tissue segmentation using semiautomated algorithms (Kollokian, 1996), and finally scaling into a standard space (Collins *et al.,* 1994). All of the above preprocessing analyses were conducted on Silicon Graphics R5000 O2 180MHZ workstations.

Reorientation. First, reslicing into a standard orientation was accomplished by trained operators "tagging" 10 standardized anatomical landmarks in each subject's image data set that corresponded to the same 10 anatomical landmarks defined on the ICBM-305 average brain (Mazziotta *et al.,* 1995). With these tag points, parameters were computed for a three-translation and three-rotation rigid-body linear transformation for each subject, and a trilinear interpolation was used to create transformed images with new isotropic 1-mm voxel dimensions. Reslicing provided image analysts with a standard view of the brain, making it easier to apply standardized rules for defining cerebral and noncerebral regions (Filipek *et al.,* 1989).

Tissue segmentation. Next, trained operators tagged samples of gray matter (40 voxels), white matter (40 voxels), ventricular CSF (20 voxels), and background (20 voxels) throughout the volume of each resliced data set. These samples were used as training sets in a tissue classification algorithm that assigned each voxel to one of the four categories. While several different tissue classification algorithms were available for these

analyses (e.g., Minimum Distance, Bayesian, *k* Nearest Neighbor, Artificial Neural Nets; Kollokian, 1996), a minimum distance classifier was chosen for this study because it provided the best results (for this T_1-weighted imaging protocol) in a qualitative analysis of the different methods. Sample tissue segmented images can be viewed in Fig. 1.

Brain masking. Tissue classified images were used to aid in creating a mask of the brain, removing scalp and other nonbrain tissues within the imaged volume. The advantage of using the tissue segmented images is that the segmented CSF around the outer edge of the cortex (in most places) could be used as a predefined border between brain and scalp. Analysts were only required to create boundaries where nonbrain tissue with signal values similar to gray or white matter was contiguous with brain tissue (see Fig. 2). After nonbrain tissue was separated, the brain mask was morphologically dilated to include subdural and ventricular CSF, thus providing estimates of total brain volume (gray and white matter only), as well as intracranial volume (including gray matter, white matter, and CSF) for each subject. Using these methods, trained image analysts can create a brain mask in roughly 1 to 1.5 h, which was a considerable time reduction over less automated techniques.

Spatial filter. Signal intensity nonuniformities caused by inhomogeneities in the scanner can result in poor classification of tissue types in different spatial regions of an imaged volume. Thus, after brain masks were created, a three-dimensional spatial filter was applied to each data set to remove low frequency changes or "drifts" in signal value across the volume. These new filtered images were then resubmitted to the minimum distance tissue classifier using the same training tag points selected earlier. Nonbrain voxels were subtracted from the new rf-corrected segmented images, and infratentorial (cerebellar and brain stem) structures were defined and subtracted.

Spatial normalization and scaling. The filtered, tissue-classified supratentorial volume from each subject was then scaled into standard ICBM-305 space using a completely automated nine-parameter linear (with scaling in the *x*, *y*, and *z* planes) spatial normalization algorithm (Collins *et al.,* 1994). Note that the spatial normalization in the "reorientation" preprocessing step consisted only of rotations in the *x*, *y*, and *z* planes with no scaling. After spatial normalization, the segmented volumes were binarized to include only voxels that segmented as gray matter for importation into the SPM96 software (Friston *et al.,* 1995).

Smoothing. The spatially normalized gray matter maps were imported into SPM96 and smoothed with an 8-mm FWHM isotropic Gaussian kernel to reduce variation due to individual differences in gyral and sulcal patterns. While other authors have chosen larger smoothing kernels for structural analyses using SPM (e.g., Shah *et al.,* 1998, 12 mm; Richardson *et al.,* 1997, 13 mm) we chose the 8-mm smoothing kernel because we thought that it best approximated the thickness of the cortex we were examining. It is also consistent with one other study in which structural gray matter differences were examined (e.g., Wright *et al.,* 1995). In their discussion of making statistical inferences, Frackowiak *et al.* (1998) state that when the "smoothing increases the probability that a large region occurs above *u* by chance increases as well" (p. 91). This suggests that our choice of an 8-mm filter is somewhat conservative relative to larger kernel sizes and is less likely to result in type I error.

Statistical analysis. First, the validity of the tissue segmentation and brain masking protocols was assessed by comparing results from the group of 19 normal control subjects analyzed using these methods and the results from analyses conducted on the same 19 subjects using an analysis protocol for the dual echo image series described by Jernigan and colleagues (Jernigan *et al.,* submitted for publication). Interrater reliability was also assessed for 10 of the 19 subjects studied. The mean errors were computed by averaging the absolute values of the differences between two measures (e.g., mean gray matter volume obtained by ERS and mean gray matter volume obtained by RB) and expressing them as a percentage of their mean.

Statistical parametric mapping was conducted for the groups of 9 children and 9 adolescents using SPM96 and two simple contrasts comparing the averaged smoothed gray matter segmentations for the younger and the older groups (child minus adolescent and adolescent minus child). Differences between groups were displayed as SPMs (Z distribution) with a voxel threshold probability of 0.001 and an extent threshold of 50 contiguous voxels per cluster. These 18 subjects were randomly assigned to groups for 20 new analyses from which the results (using the same height and extent thresholds as the group tests) were tabulated to assess the overall significance of the SPM.

Next, chronological age was used as a continuous variable in two multisubject single covariate-of-interest statistical analyses (negative age effects and positive age effects). The covariate (age) effects were estimated at each voxel to obtain SPM[Z] maps with a voxel threshold probability of 0.001 and an extent threshold of 50 contiguous voxels.

Each data set was segmented using samples of gray matter, white matter, and CSF tagged within each independent volume resulting in new segmented images where global differences in signal value from the raw data were no longer relevant. All subsequent analyses were run on the classified data. Thus, corrections for global differences in gray matter density or signal value (global normalization), that are typically
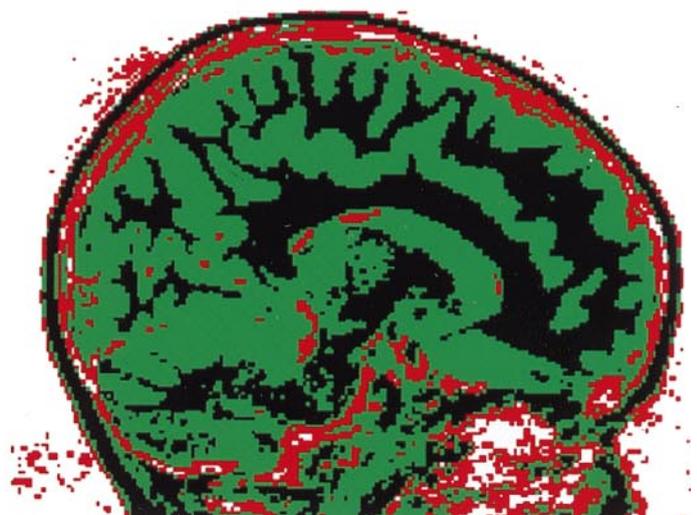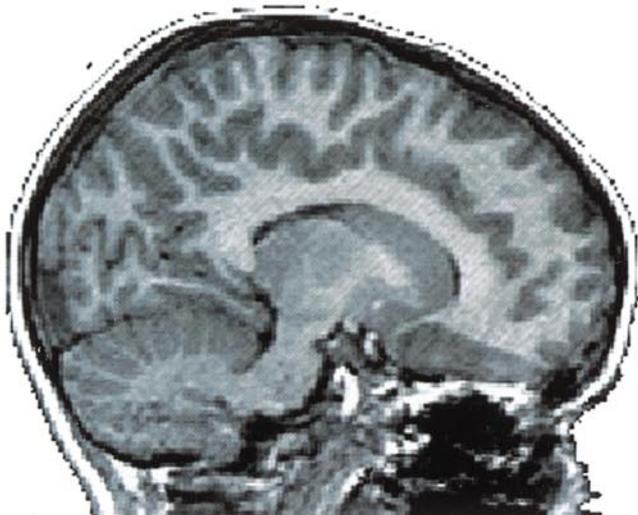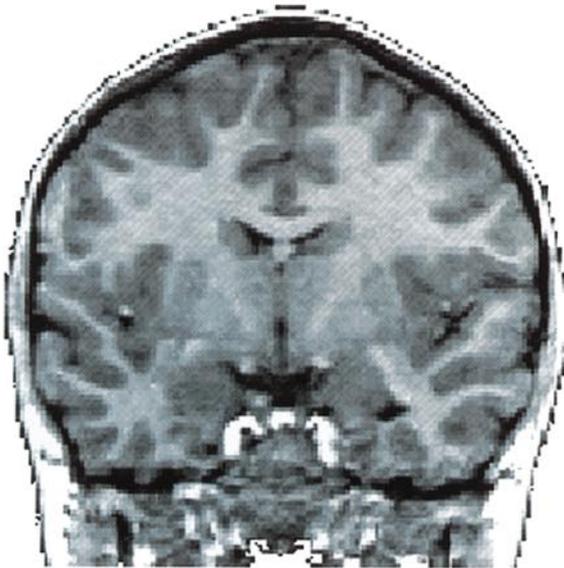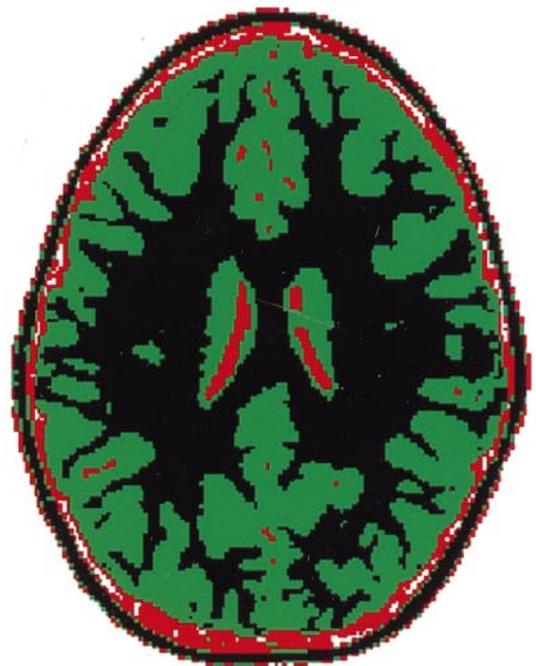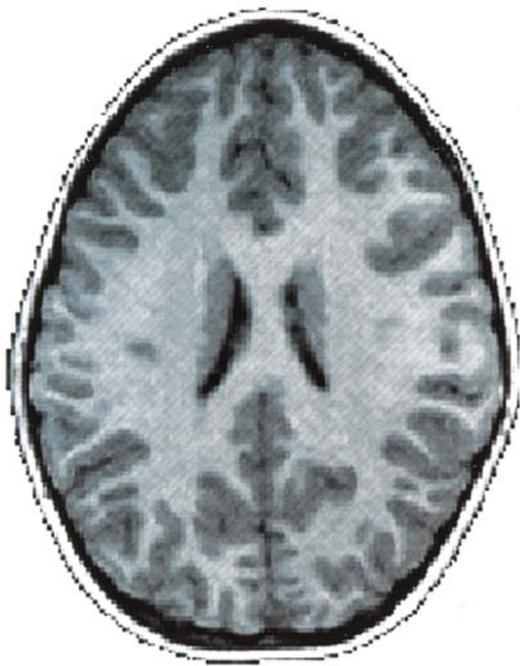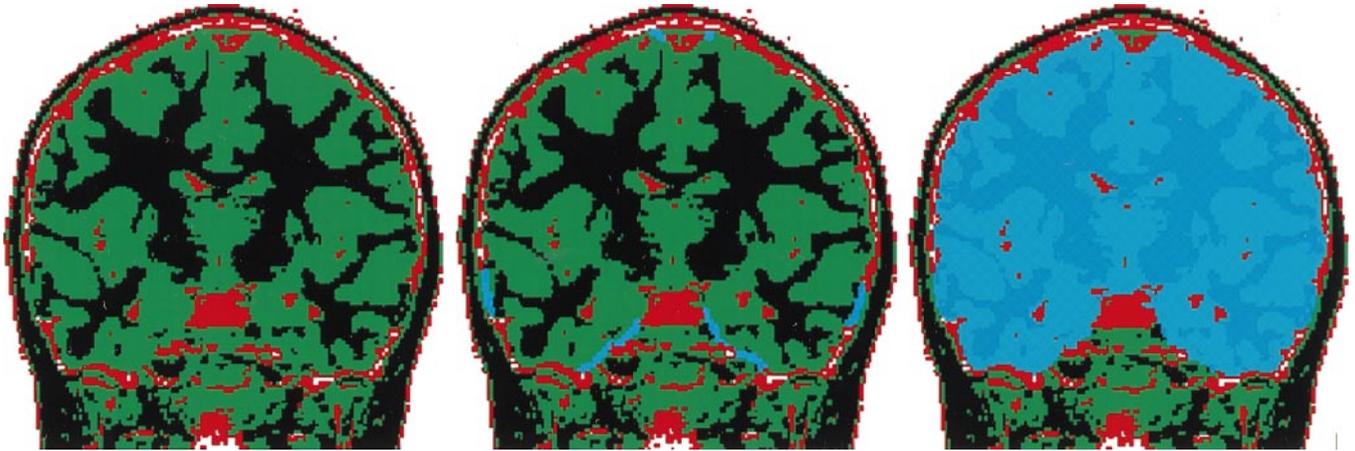
FIG. 2. Tissue-segmented image undefined (left), image with gray and white matter pixels which are contiguous with nonbrain pixels designated in light blue (middle), and complete brain region filled in light blue for one sample slice (right).

used with functional imaging data sets, were not applied for the statistical parametric analyses because gray matter "density" was no longer a characteristic of the data (e.g., tissue segmentation yielded data sets where gray matter voxels within a range of densities were collapsed into one category throughout each volume).

To test the regional hypotheses that relatively more significant differences would be observed in dorsal frontal and parietal regions and relatively few would be observed in the ventral cortices and mesial structures, several brain regions were defined on an average of all subjects spatially normalized image data sets. First, subcortical gray matter (including caudate, putamen, globus pallidus, and mesial septal basal forebrain structures) was separated from the cortical structures. Four cortical quadrants were defined stereotaxically based on two planes, one axial plane (perpendicular to the midsagittal plane) passing through the most anterior point in the genu and the most posterior point in the splenium of the corpus callosum and one coronal plane (perpendicular to the axial plane) passing through the midpoint between the anterior and posterior commissures. The four new quadrants were: (1) inferior to the axial plane and anterior to the coronal plane, (2) inferior to the axial plane and posterior to the coronal plane, (3) superior to the axial plane and anterior to the coronal plane, and (4) superior to the axial plane and posterior to the coronal plane. Note that each new quadrant consisted of gray matter, white matter, and CSF that was not previously defined within the subcortical region described above. Statistical significance for each quadrant and the subcortical region was assessed by counting the number of significant voxels from the

group SPM analysis that fell into each region. This distribution of voxels was compared to the null hypothesis (that all quadrants and the subcortical region would have an equal number of significant voxels) using a χ^2 test. Because regions differed in gray matter volume, each voxel count was expressed as a ratio to that of the total average gray matter volume in the region from which it was measured.

RESULTS

Statistical parametric mapping. For all statistical parametric analyses, a height threshold probability of 0.001 and an extent threshold of 50 contiguous voxels were used to assess for statistical significance.

Localized differences in gray matter between the group of nine children and the group of nine adolescents are displayed as SPM[Z] maps in Figs. 3A and 3B. The SPM representative of gray matter loss between childhood and adolescence (e.g., child minus adolescent) can be seen in Fig. 3A. When the same height and extent thresholds were used to assess gray matter increases between childhood and adolescence (e.g., adolescent minus child), no significant voxels were observed. As shown in Fig. 3B, when a less stringent height threshold was used ($P = 0.005$), one significant cluster was revealed.

Results from the regional hypotheses (of gray matter losses; Fig. 3A) indicate that the pattern of significant voxels (relative to total regional gray matter volume) is not uniform across all five anatomical regions ($\chi^2 = 160$, $df = 4$; $P < 0.001$). As predicted, the dorsal cortices of the frontal and parietal regions were much more variable with age than were the ventral or subcortical regions. The parietal region had more significant voxels than the frontal region ($\chi^2 = 8.5$, $df = 1$, $P < 0.01$). The distribution of significant voxels for each of the five regions can be seen in Table 1, and Table 2 contains a

FIG. 1. Sample original T_1-weighted and tissue segmented images.

Group Comparison SPM{Z} Map
Grey Matter Loss

A

p < .001, Extent
{k} = 50
Uncorrected

Group Comparison SPM{Z} Map
Grey Matter Gain

B

p < .005, Extent
{k} = 50
Uncorrected
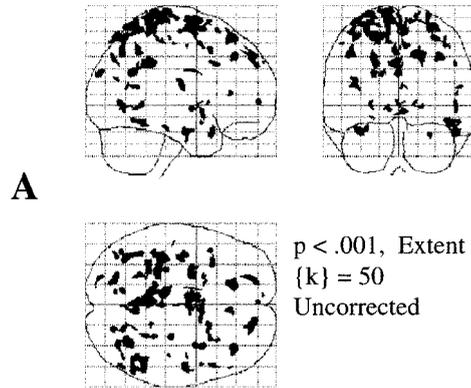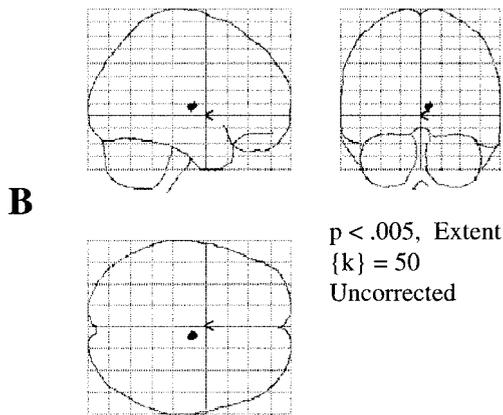
FIG. 3.   (A) SPM[Z] map of the group effect of gray matter loss representing the contrast: children minus adolescents. (B) SPM[Z] map of the group effect of gray matter gain representing the contrast: adolescents minus children.

TABLE 1

Ratio of Significant Voxels from the Group Difference SPM to the Total Average Gray Matter in Each of Five Regions

	Region gray matter in voxels	Significant voxels	Voxels/ region
Inferior anterior (orbital frontal and anterior temporal)	205,689	291	0.0014
Inferior posterior (occipital and posterior temporal)	186,002	304	0.0016
Superior anterior (dorsal frontal)	284,759	1867	0.0065
Superior posterior (parietal)	390,413	4034	0.0103
Subcortical	68,667	66	0.0010

Fig. 5A. When the same height and extent thresholds were used to assess gray matter increases with increasing age (e.g., positive age effects), no significant voxels were observed. As shown in Fig. 5B, when a less stringent height threshold was used ($P = 0.005$), one significant cluster was revealed.

Figure 6 is a graphical display of the age effect for one highly significant voxel from the covariance of interest analysis. As can be seen, the older subjects have a lower signal value (more similar to white matter) at that voxel location than do their younger counterparts. In Fig. 7, the significant clusters for both the covariance (negative age effects; in red) and the group tests (child minus adolescent; in green) for age effects can be seen mapped onto three sequential left hemisphere sagittal sections for the average younger and average older subjects. Note the dramatic change in appearance and perhaps posterior relocation of the marginal arm of the left cingulate sulcus between childhood and adolescence revealed with these analyses.

list of Talairach coordinates for the most significant voxel within each of the 10 largest clusters from the group analyses (child minus adolescent contrast).

To assess the overall significance of the omnibus group test, subjects were randomly assigned to groups in 20 new analyses. The mean number of significant clusters for the 20 randomized tests was 5.8 (SD = 6, range 0 to 26), compared to the 57 significant clusters in the omnibus group test ($P < 0.05$; permutation test). Figure 4 contains two representative randomized SPMs.

The covariate (age) effects were estimated at each voxel to obtain SPM[Z] maps for the two contrasts (positive age effects and negative age effects). The results of these analyses were similar, but not identical, to those for the group difference tests discussed above. The SPM representative of gray matter loss with increasing age (e.g., negative age effects) can be seen in

TABLE 2

Talairach Coordinates of the Most Significant Voxel within the 10 Largest Clusters in the Group Contrast (Child Minus Adolescent)

| Cluster size in voxels	Talairach coordinates (mm)		
	x	y	z
1104	−7	0	72
1015	−1	−58	27
982	−27	−35	76
902	−11	−42	67
613	−38	−64	57
558	1	−31	72
489	−35	−45	67
455	44	−57	−12
449	30	−61	65
395	−22	−73	57

Segmentation validity. Volumetric results obtained using these tissue segmentation methods were very similar to the results obtained in another laboratory (Jernigan *et al.,* under review) when the same 19 subjects were examined. The Pearson correlations for total gray, white, and CSF volumes obtained using the two methods were 0.88, 0.88, and 0.83, respectively. The correlation for total brain volume obtained by the two laboratories was 0.99.

Segmentation reliability. Interrater reliability measures for gray matter, white matter, and CSF volumes obtained for 10 subjects by two experienced image analysts (authors E.R.S. and R.B.) were high. Pearson correlation coefficients were 0.98 for gray matter, 0.96 for white matter, and 0.94 for CSF. Error estimates were 1% for gray matter and 2% for white matter and CSF. The variability between raters for these measures arises from differences in tag point selection.

DISCUSSION

The goal of this study was to localize maturational changes in brain morphology between childhood and
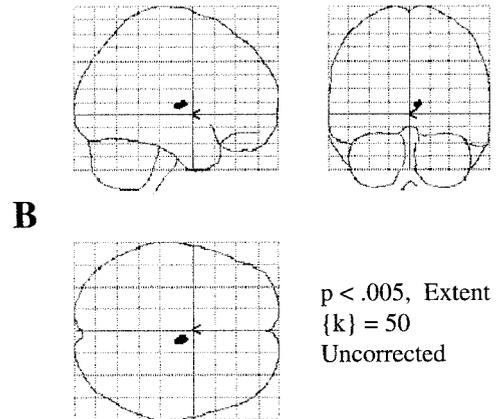
Random Group Assignment SPM{Z} Maps

p < .001, Extent {k} = 50
Uncorrected

p < .001, Extent {k} = 50
Uncorrected
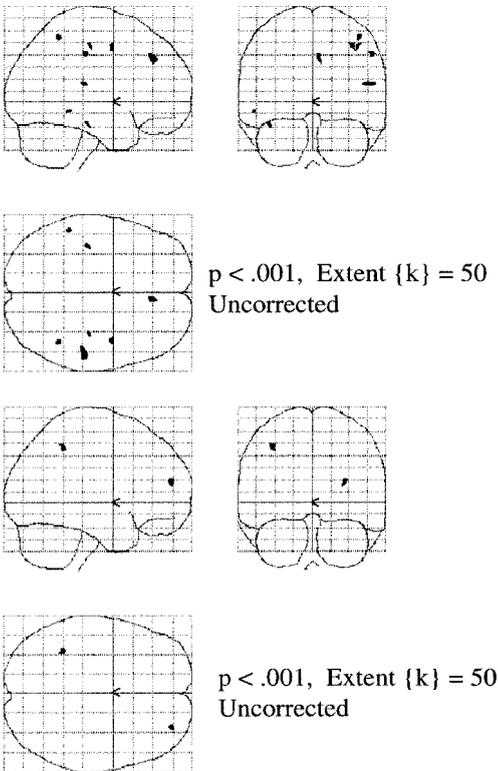
FIG. 4. SPM{Z} maps of two representative randomized group tests.

Age as a Covariate of Interest
SPM{Z} Map: Grey Matter Loss

A

p < .001, Extent {k} = 50
Uncorrected

Age as a Covariate of Interest
SPM{Z} Map: Grey Matter Gain

B

p < .005, Extent {k} = 50
Uncorrected
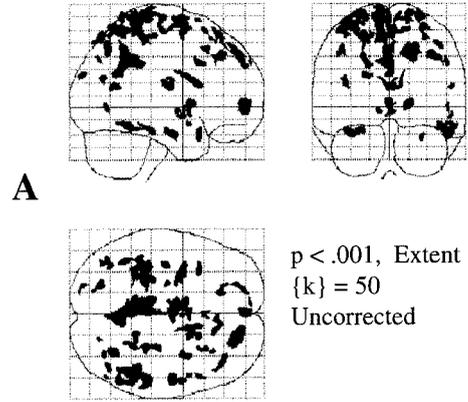
FIG. 5. (A) SPM{Z} map of the covariate of interest analysis for the contrast assessing the negative effects of age. (B) SPM{Z} map of the covariate of interest analysis for the contrast assessing the positive effects of age.

adolescence by testing for age effects on a voxel by voxel basis using parametric statistics. As predicted, more age-related differences in the SPMs were seen in the dorsal cortices of the frontal and parietal lobes whether group differences or continuous age effects were assessed. The most dramatic changes appear to be occurring in parietal cortices and seem to result from regions on the border between gray and white matter that are changing from gray matter signal in the younger subjects to white matter signal in the older subjects. Such effects would be expected given that myelin deposition continues to occur throughout the age range studied here, and the association cortices of frontal and parietal regions are known to myelinate later than cortices in more ventral brain regions (Yakovlev and Lecours, 1967). Changes that seem to result from subtle movement or relocation of some sulci between
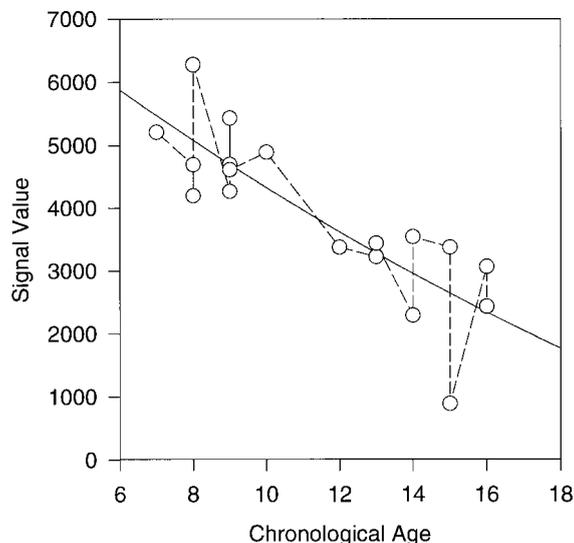
FIG. 6. Scatterplot of signal value by chronological age (at Talairach coordinate −35, −69, 20) for one highly significant voxel from the covariance analysis (negative age effects).

childhood and adolescence (e.g., posterior relocation of marginal arm of cingulate sulcus in the left hemisphere) have not previously been noted in the literature, and further studies are under way to address this possibility.

Interrater reliabilities for tissue segmentation of gray matter, white matter, and CSF were all 0.94 and above using these methods. These correlation coefficients are considerably higher than reported reliability (0.81) from another group doing similar studies with tissue classification and SPM (e.g., Wright *et al.,* 1995). The results obtained using this tissue segmentation protocol for the high-resolution T$_1$-weighted images were comparable to the results obtained for the same subjects when analyzing a dual echo series and using a more sophisticated tissue classification algorithm (Jernigan *et al.,* submitted for publication). While the dual echo series probably yields more accurate tissue segmentation (Clark *et al.,* 1995), the tradeoff for an increase in spatial resolution with the single T$_1$-weighted series is crucial for this type of study where localization is the goal. Additionally, in a regression analysis, the age effects for total gray matter were highly significant for volume reduction (β = −0.35, $P < 0.001$) when brain size was also taken into account as a covariate. These results are virtually identical to the age effects observed for total gray matter volume (relative to total brain volume) when the dual echo protocol was used (Sowell *et al.,* submitted for publication). Given these findings, it seems that multispectral imaging protocols, which are typically lower in spatial resolution, could be exchanged for high-resolution single-spectrum T$_1$-weighted imaging protocols, particularly in relatively

young subjects where gray/white contrast is reasonably high.

As seen in the SPMs, the original hypotheses of this study (that the distribution of significant clusters would roughly parallel the pattern of results observed in the volumetric studies of the same subjects) are supported. The relatively subtle effects of continuing myelination and regressive maturational factors that occur throughout adolescence can be localized using these methods. It should be noted, however, that the sample size studied here was relatively small, and the generalizability of the results is not known. Assessment of gender differences in the age effects may also be relevant, but could not be assessed here due to the small sample size. Nonetheless, the significant findings are valid in this sample, providing further evidence that the human cerebral cortex does mature in a regionally and temporally variable progression throughout adolescence.

The significance level for the clusters in the SPMs was determined by permutation tests, rather than by using the theory of Gaussian random fields, since fewer assumptions about the signal are required by the nonparametric test. The multiple comparison correction factors in SPM96 are inappropriately stringent for this type of study because of the presence of higher spatial frequencies in structural maps relative to functional activation maps. In functional imaging studies, researchers analyze significance by using nonparametric approaches (e.g., permutation test) or by making additional assumptions (e.g., signal can be modeled as a smooth Gaussian random field). By making the additional assumptions, an approximate P value for the effect is obtained at the expense of possibly overcorrecting the significance level. Permutation tests are preferable because they require fewer assumptions (Bullmore *et al.,* 1996), although they are time consuming and computationally intensive.

The age effects observed here resulted from signal values that decrease with increasing age, as would be expected given the findings from volumetric studies. In other words, the younger children had signal values more representative of gray matter in dorsal frontal and parietal regions, and the adolescents had signal values more representative of white matter in these regions. Notably, the results varied somewhat depending on the design of the statistical analysis. The regional distribution of age effects in both group and covariance analyses appeared quite similar, but subtle

FIG. 7. Three left hemisphere sagittal sections from the average brain of the young children (left column) and the corresponding sagittal slices for the average brain of the adolescents (right column). Highlighted in green are the clusters that were significant in the group analysis (child minus adolescent, $P < 0.001$) and in red are the clusters which were significant in the covariance analysis (negative age effects, $P < 0.001$).
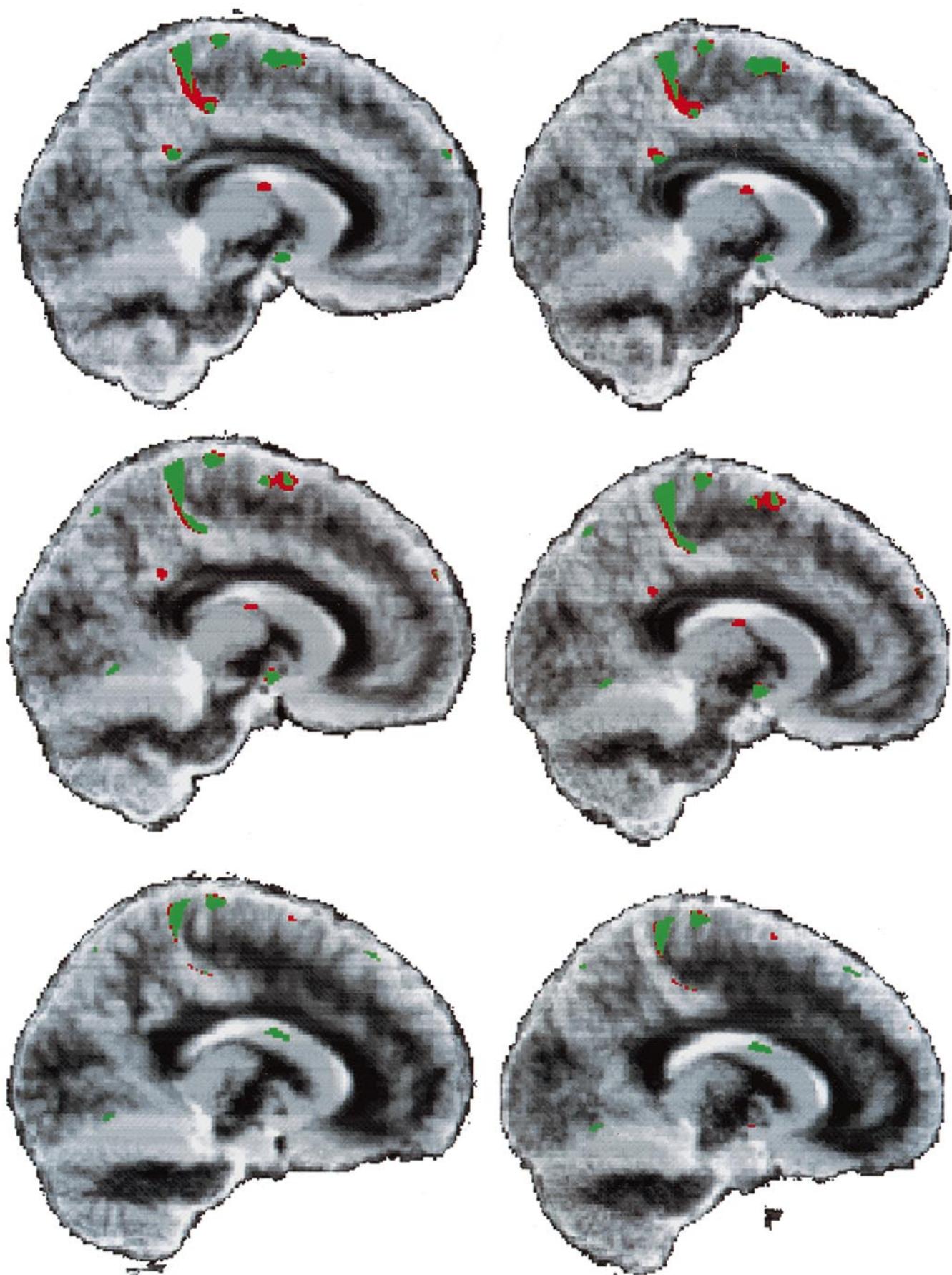
differences in the spatial location and size of the significant clusters suggest that the two types of analyses might tap different aspects of maturation. This is not surprising given that we would expect the effects we are measuring to be somewhat phasic, or nonlinear, in nature. That is, we originally chose the two age groups to be roughly pre- and postpubertal, and factors known to affect brain morphology (e.g., pubertal/hormonal) which occur sometime between the ages of the younger and older groups studied here are presumed to be related to the changes measured (see Garcia-Segura, 1994, for a review of the role of gonadal hormones in brain structural plasticity). However, the subject assignment for the group test may not have been optimal for separating "pubertal" phases, and it is possible that if the ages had been distributed differently for the two groups (e.g., 7 to 12 years for the children and 14 to 16 years for the adolescents), slightly different results would have been observed. Thus, we believe that the group test was more reflective of nonlinear aspects of the age effects that could not be observed with the linear covariance analysis.

Interestingly, the age effects/group differences observed here appear to be most prominent in parietal regions in this age range, despite postmortem (Yakovlev and Lecours, 1967) and functional studies (Chugani and Phelps, 1986) showing evidence for a caudal to rostral and posterior to anterior progression of maturational changes. One might expect dorsal frontal regions to be the most variable across this age range given the above findings. However, results from volumetric studies (Sowell *et al.,* submitted for publication) actually show more robust changes in parietal than frontal cortices in these subjects, which is consistent with the results observed from SPM. Clearly, the progressive and regressive events are distributed temporally as well as spatially, and perhaps frontal regions are maturing somewhat later (between adolescence and adulthood) than the parietal regions; further studies to assess this issue are under way.

Methods employed in this study to normalize the children's brains into a standard space (ICBM-305) may or may not be appropriate for a developmental population. Morphological changes in the brain throughout development are increasingly observed to be regionally heterogeneous (Jernigan *et al.,* 1991; Sowell and Jernigan, 1999), and the brain does not appear to finish growing completely until late adolescence (e.g., Sowell *et al.,* submitted for publication). Thus, linear warping techniques may differentially over- or underestimate actual changes depending on whether the region under study is in a static or plastic developmental phase. Nonlinear warping algorithms may be more appropriate for the study of a population where the brain is not yet completely developed (for a discussion, see Toga *et al.,* 1997). An additional limitation to using linear warping algorithms is that anatomical variability tends to be greater in lateral neocortices than in the mesial subcortical region. This tends to result in regionally variable power to detect differences between groups or with age such that lateral changes are less likely to be observed than mesial changes. Nonetheless, the findings here parallel those from other morphometric studies where the children's brains were not warped or scaled outside native space (Jernigan *et al.,* 1991; Sowell *et al.,* submitted for publication), and the significant findings were disproportionately in the lateral cortices where we should have the least power to find significant effects. This suggests that valid information can be obtained from the linear warping algorithm used here, but further studies are under way to address these important issues.

While the SPM analysis was developed specifically to examine functional activation, this study of normal brain maturation suggests that it has utility in assessing relatively subtle structural changes as well. Results from the SPM analyses were consistent with the findings from volumetric assessments of the same subjects. These methods may be useful for more exploratory analyses of brain morphology in rare developmental populations where relatively little is known about aberrant brain structure.

ACKNOWLEDGMENTS

REFERENCES

Andraesen, N. C., Arndt, S., Swayze, V., Cizadlo, T., Flaum, M., O'Leary, D., Ehrhardt, J. C., and Yuh, W. T. 1994. Thalamic abnormalities in schizophrenia visualized through magnetic resonance image averaging. *Science* **266**(5183):294–298.

Bullmore, E., Brammer, M., Williams, S. C. R., Rabe-Hesketh, S., Janot, N., David, A., Mellers, J., Howard, R., and Sham, P. 1996. Statistical methods of estimation and inference for functional MR image analysis. *Magn. Reson. Med.* **35**(2):261–277.

Caviness, V. S., Kennedy, D. N., Richelme, C., Rademacher, J., and Filipek, P. A. 1996. The human brain age 7–11 years: A volumetric analysis based on magnetic resonance images. *Cereb. Cortex* **6**:726–736.

Chugani, H. T., and Phelps, M. E. 1986. Maturational changes in cerebral function in infants determined by [18]FDG positron emission tomography. *Science* **231**:840–843.

Clark, L. P., Velthuizen, R. P., Camacho, M. A., Heine, J. J., Vaidyanathan, M., Hall, L. O., Thatcher, R. W., and Silbiger, M. L. 1995. MRI segmentation: Method and applications. *Magn. Reson. Imag.* **13**(3):343–368.

Collins, D. L., Neelin, P., Peters, T. M., and Evans, A. C. 1994. Automatic 3D intersubject registration of MR volumetric data in standardized Talairach space. *J. Comput. Assist. Tomogr.* **18**(2):192–205.

Filipek, P. A., Kennedy, D. N., Caviness, V. S., Jr., Rossnick, S. L., Spraggins, T. A., and Starewics, P. M. 1989. Magnetic resonance imaging-based bran morphometry: Development and application to normal subjects. *Ann. Neurol.* **25**(1):61–67.

Frackowiak, R. S. J., Friston, K. J., Frith, C. D., Dolan, R. J., and Mazziotta, J. C. 1998. *Human Brain Function,* pp. 85–106. Academic Press, San Diego.

Friston, J. K., Holmes, A. P., Worsley, K. J., Poline, J. B., Frith, C. D., and Frackowiak, R. S. 1995. Statistical parametric maps in functional imaging: A general approach. *Hum. Brain Map* **2**:189–210.

Garcia-Segura, L. M., Chowen, J. A., Parducz, A., and Naftolin, F. 1994. Gonadal hormones as promoters of structural synaptic plasticity: Cellular mechanisms. *Prog. Neurobiol.* **44**:279–307.

Giedd, J. N., Snell, J. W., Lange, N., Rajapakse, J. C., Casey, B. J., Kozuch, P. L., Vaituzis, A. C., Vauss, Y. C., Hamburger, S. D., Kaysen, D., and Rapoport, J. L. 1996a. Quantitative magnetic resonance imaging of human brain development: Ages 4–18. *Cereb. Cortex* **6**:551–560.

Giedd, J. N., Vaituzis, A. C., Hamburger, S. D., Lange, N., Rajapakse, J. C., Kaysen, D., Vauss, Y. C., and Rapoport, J. L. 1996b. Quantitative MRI of the temporal lobe, amygdala, and hippocampus in normal human development: Ages 4–18 years. *J. Comp. Neurol.* **366**:223–230.

Huttenlocher, P. R. 1979. Synaptic density in human frontal cortex: Developmental changes and effects of aging. *Brain Res.* **163**:195–205.

Huttenlocher, P. R., and de Courten, C. 1987. The development of synapses in striate cortex of man. *Hum. Neurobiol.* **6**:1–9.

Jernigan, T. L., Trauner, D. A., Hesselink, J. R., and Tallal, P. A. 1991. Maturation of the human cerebrum observed *in vivo* during adolescence. *Brain* **114**:2037–2049.

Jernigan, T. L., Archibald, S., Foster, D., Fennema-Notestine, C., Sellers, J., Symonds, L., Harris-Collazo, M., Philipsen, P., Stout, J., Ryan, L., Corey-Bloom, J., Sowell, E. R., and Hesselink, J. 1999. Reliability of methods for anatomical labeling of structural magnetic resonance image volumes. Submitted for publication.

Kollokian, V. 1996. *Performance Analysis of Automatic Techniques for Tissue Classification in Magnetic Resonance Images of Human Brain,* masters thesis. Concordia University, Department of Computer Science, Montreal, Quebec, Canada.

Mazziotta, J. C., Toga, A. W., Evans, A., Fox, P., and Lancaster, J. 1995. A probabilistic atlas of the human brain: Theory and rationale for its development—The International Consortium for Brain Mapping. *NeuroImage* **2**(2):89–101.

Pfefferbaum, A., Mathalon, D. H., Sullivan, E. V., Rawles, J. M., Zipursky, R. B., and Lim, K. O. 1994. A quantitative magnetic resonance imaging study of changes in brain morphology from infancy to late adulthood. *Arch. Neurol.* **51**:874–887.

Reiss, A. L., Abrams, M. T., Singer, H. S., Ross, J. L., and Denckla, M. B. 1996. Brain development, gender and IQ in children: A volumetric imaging study. *Brain* **119**:1763–1774.

Richardson, M. P., Friston, K. J., Sisodiya, S. M., Koepp, M. J., Ashburner, J., Free, S. L., Brooks, D. J., and Duncan, J. S. 1997. Cortical grey matter and benzodiazepine receptors in malformations of cortical development. A voxel-based comparison of structural and functional imaging data. *Brain* **120**(11):1961–1973.

Shah, P. J., Glabus, M. F., Goodwin, G. M., and Ebmeier, K. P. 1998. Cortical grey matter reductions associated with treatment resistant chronic unipolar depression: A controlled MRI study. *Br. J. Psychiatry,* **172**:527–32.

Sled, J. G., Zijdenbos, A. P., and Evans, A. C. 1998. A nonparametric method for automatic correction of intensity nonuniformity in MRI data. *IEEE Trans. Med. Imag.* **17**(1):87–97.

Sowell, E. R., and Jernigan, T. L. 1999. Further MRI evidence of late brain maturation: Limbic volume increases and changing asymmetries during childhood and adolescence. *Dev. Neuropsychol.,* **14**(14):599–617.

Sowell, E. R., Trauner, D. A., Thomas, R. G., and Jernigan, T. L. (Submitted). Age–related changes in brain structure during late childhood and early adulthood: A structural magnetic resonance imaging study.

Toga, A. W., Thompson, P. M., and Payne, B. A. 1997. Modeling morphometric changes of the brain during development. In *Developmental Neuroimaging: Mapping the Development of Brain and Behavior* (R. W. Thatcher, G. Ried Lyon, J. Rumsey, and N. Krasnegor, Eds.), pp. 15–27. Academic Press, San Diego.

Wright, I. C., McGuire, P. K., Poline, J.-B., Travere, J. M., Murray, R. M., Frith, C. D., Frackowiak, R. S. J., and Friston, K. J. 1995. A voxel-based method for the statistical analysis of gray and white matter density applied to schizophrenia. *NeuroImage* **2**:244–252.

Yakovlev, P. I., and Lecours, A. R. 1967. The myelogenetic cycles of regional maturation of the brain. In *Regional Development of the Brain in Early Life* (A. Minkowski, Ed.), pp. 3–70. Blackwell, Oxford.

Zecevic, N., and Rakic, P. 1991. Synaptogenesis in monkey somatosensory cortex. *Cereb. Cortex* **1**(6):510–523.